Tellurium(II) Dialkanethiolates: $n_p(S)$-σ*(Te−S′) Orbital Interactions Determine the ^{125}Te NMR Chemical Shift, and the Molecular and Crystal Structure

Holger Fleischer,*[a] Norbert W. Mitzel,[b] and Dieter Schollmeyer[c]

Keywords: NMR spectroscopy / Noncovalent interactions / Solid-state structures / Sulfur / Tellurium

Tellurium(II) dimethanethiolate, $Te(SMe)_2$, and tellurium(II) diethanethiolate, $Te(SEt)_2$, were synthesized by reaction of TeO_2 and $Te(OiPr)_4$ with HSMe and HSEt, respectively. In the solid state, $Te(SMe)_2$ exhibits a *cis*-conformation of the methyl groups with respect to the TeS_2 plane – an unprecedented situation for nonfunctionalized organotrichalcogenides – whereas $Te(SEt)_2$ shows a *trans*-conformation. Ab initio calculations performed for $Te(SMe)_2$ and $Te(SEt)_2$ show that the *cis*- and *trans*-conformers represent minima on the potential energy surface and are stabilized by intramolecular π-type n(S)-σ*(Te–S′) orbital interactions. In the solid state, the molecules of each compound are associated through two centrosymmetric Te_2S_2 units with two of their neighbors, resulting in tetracoordinate Te atoms with distorted trapezoidal configurations. While the intermolecular Te···S distance increases in the sequence R = Me < Et < *i*Pr < *t*Bu, the length of the covalent Te–S bond decreases in the same order, a result attributed to intermolecular σ-type $n_p(S)$-σ*(Te–S′) orbital interactions. The ^{125}Te NMR chemical shift of $Te(SR)_2$ largely depends on R (R = Me, Et, *i*Pr, *t*Bu) and shows a nearly linear correlation with the first ionization energy of the corresponding thiol HSR. Ab initio calculations of the ^{125}Te NMR shifts for the model compound $Te(SH)_2$ (C_2 symmetry) reveal that it also depends strongly on the HSTeS torsion angle. These results can be explained by a model in which π-type $n_p(S)$-σ*(Te–S′) and $n_p(Te)$-σ*(S–H) orbital interactions determine the paramagnetic shielding of the tellurium nucleus.

Introduction

In nearly every case known so far, noncyclic diorganotrichalcogenides, $RE^1E^2E^3R$ (see Scheme 1), exhibit a helical structure, as is the case in hexagonal selenium or tellurium, i.e. both R groups are *trans* with respect to the $E^1E^2E^3$ plane.[1−5] Spectroscopic and quantum chemical investigations have clearly demonstrated that trisulfane, HSSSH, can exist as both the *cis*- and *trans*-conformer. Due to the small steric demand of the hydrogen atoms, their energies differ by only 1 kJ·mol^{-1} in favor of the *trans*-conformer.[6,7]

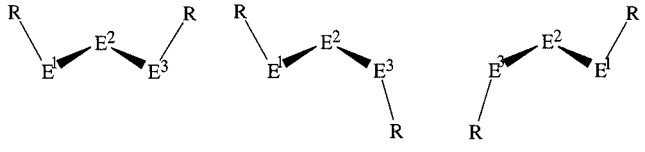

Scheme 1. Structural formulae of the organotrichalcogenides with *cis*- (left) and two enantiomeric *trans*- (middle and right) conformations (R = organic group, E^1, E^2, E^3 = S, Se, Te)

Tellurium(II) dithiolates, $Te(SR)_2$, are thermally and photochemically unstable with respect to decomposition to elemental tellurium and disulfide, RSSR, but their kinetic stability depends very much on R.[3,8] This class of compounds is thus a source of elemental tellurium, whose release and deposition on surfaces can be controlled by thermal energy and irradiation. Recent ab initio studies have shown that the kinetic stability is due to the conformation of the CSTeS unit, which, in turn, is likely to be a consequence of π-type $n_p(S^1)$-σ*(Te−S^2) orbital interactions.[8] The motivation of the present research was to synthesize sterically noncrowded tellurium(II) dithiolates, $Te(SR)_2$, and to investigate their stability, physical properties and structural features.

Results and Discussion

Synthesis

$Te(SMe)_2$ and $Te(SEt)_2$ were prepared by reductive elimination from Te^{IV} compounds according to Equations (1) and (2):

[a] Institut für Anorganische Chemie und Analytische Chemie, Johannes Gutenberg Universität Mainz,
Duesbergweg 10−14, 55099 Mainz, Germany
Fax: (internat.) + 49-(0)6131/3923351
E-mail: fleische@mail.uni-mainz.de
[b] Institut für Anorganische und Analytische Chemie, Westfälische Wilhelms-Universität Münster
48149 Münster, Germany
[c] Institut für Organische Chemie, Johannes Gutenberg Universität Mainz
Duesbergweg 10−14, 55099 Mainz, Germany

$$TeO_2 + 4\ MeSH \rightarrow Te(SMe)_2 + (SMe)_2 + 2\ H_2O \quad (1)$$

$$Te(O\mathit{i}Pr)_4 + 4\ EtSH \rightarrow Te(SEt)_2 + (SEt)_2 + 4\ HO\mathit{i}Pr \quad (2)$$

Both compounds form yellow crystals giving dark red liquids on melting. They are stable towards air and water, but, like other tellurium(II) dithiolates,[4] are thermodynamically unstable towards decomposition to Te and the respective disulfides. They are kinetically much less stable than $Te(S\mathit{i}Pr)_2$ and $Te(S\mathit{t}Bu)_2$ and, within a few hours, the walls of glass flasks containing one of the compounds at room temperature are covered by a thin, mirror-like film of tellurium. $Te(SMe)_2$ and $Te(SEt)_2$ are also very sensitive to light, and in order to minimize decomposition the compounds were kept in the dark at −40 °C.

Like $Te(S\mathit{i}Pr)_2$ and $Te(S\mathit{t}Bu)_2$, $Te(SMe)_2$ and $Te(SEt)_2$ exchange their thiolate ligands with thiols and other tellurium(II) dithiolates.[4] On the other hand, cryoscopic measurements hint at $Te(SMe)_2$ being monomeric in cyclohexane solution, which means that intermolecular associations are rather weak (vide infra).

NMR Spectroscopy

In contrast to the compounds $Te(OR)_4$, whose ^{125}Te NMR chemical shifts vary only slightly with R, $\delta[^{125}Te(SR)_2]$ depends strongly on R, as can be seen from the data given in Table 1. A major influence of inductive electronic effects or of through-space shielding of the groups R on $\delta(^{125}Te)$ can hence be excluded, since in these cases, the four ligands in $Te(OR)_4$ should have a stronger effect than the two ligands in $Te(SR)_2$. Thus, $\delta[^{125}Te(SR)_2]$ must largely be determined by stereoelectronic effects and should therefore depend on the C−S−Te−S torsion angle. Indeed, ab initio NMR calculations performed in the present study for the model compound $Te(SH)_2$ (C_2 symmetry) revealed a strong dependence of $\delta(^{125}Te)$ on τ(H−S−Te−S), while $\delta[^{125}Te(OH)_4]$ (C_2 symmetry) varies only slightly with $\tau(HO^{eq}TeO^{eq})$ (see Figure 1 and Table 2). For $Te(SH)_2$, the shielding of the ^{125}Te nucleus is at its maximum, i.e. $\delta(^{125}Te)$ is a minimum, if τ(H−S−Te−S) = 90°.[12] Figure 2 shows the nearly linear correlation between $\delta[^{125}Te(SR)_2]$ and the first ionization energy of the corresponding thiol. A theoretical model for these results is presented in terms of natural orbitals and their interaction;[12,13] the relevant data are given in Table 2. The chemical shift of the heavier elements is mainly determined by the paramagnetic contribution to the nuclear shielding, σ_p. In terms of the MO concept, σ_p is proportional to the reciprocal of the energy difference, ΔE, between the highest occupied and the lowest unoccupied MO to which the AOs of the atom considered make a substantial contribution.[14] Hence, the bigger ΔE, the smaller is σ_p and the more the signal is shifted to high field. In terms of localized natural bond orbitals (NBO), the HOMO is mainly represented by the n_p(Te) orbital and the LUMO by the symmetric combination of both σ*(Te−S) orbitals. Nevertheless, a second-order perturbation analysis revealed significant n_p(Te)-σ*(S−H) and n_p(S)-σ*(Te−S′) orbital interactions. According to second-order perturbation theory, the energy of n_p(Te), and thus of the HOMO, is lowered and the energy of σ*(Te−S), and thus of the LUMO, is raised by these interactions. The data given in Table 2 confirm that E_{HOMO} correlates with $E[n_p(Te)\text{-}\sigma^*(S-H)]$ and E_{LUMO} with $E[n_p(S)\text{-}\sigma^*(Te-S')]$. Hence, the energies of HOMO and LUMO also show a strong dependence on τ(HSTeS) and support the model that their difference is essential for $\delta(^{125}Te)$. With Koopman's theorem,[15] the dependence of $\delta(^{125}Te)$ on the first ionization energy of the corresponding thiol can be rationalized. According to this theorem, the first ionization energy of a molecule is equal to the negative energy of its HOMO, i.e. n_{3p}(S) in the case of the thiols. Second-order perturbation theory predicts an increased $n_p(S)\text{-}\sigma^*(Te-S')$ interaction if $E[n_{3p}(S)]$ is raised and hence IE(HSR) is lowered. This has the effect that E_{LUMO} and ΔE are increased and thus $\delta(^{125}Te)$ is decreased, in accordance with the results presented in Figure 1 and 2.[16]

Table 1. ^{125}Te NMR chemical shifts of tellurium(II) dialkanethiolates and tellurium(IV) tetraalkoxides, calculated values are given in parentheses[9]

	R = Me	R = Et	R = *i*Pr	R = *t*Bu
$Te(SR)_2$	1419 (1376) [a]	1184 (1319)[a]	1026 [b]	907 (883) [a,b]
$Te(OR)_4$	1519 (792) [a] [c]	1503 [d]	1538 [c]	–

[a] Calculated value for conformer with C_2 symmetry. [b] Value from reference.[4] [c] Value from reference.[10] [d] Value from reference.[11]

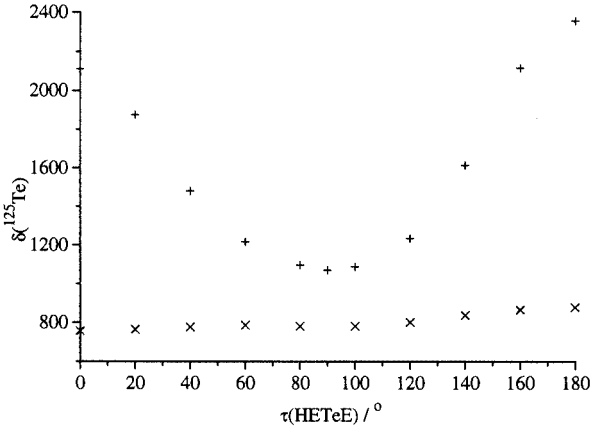

Figure 1. HF/3−21G(d) calculated ^{125}Te NMR chemical shifts of $Te(SH)_2$ (+, C_2 symmetry, MP2/LANL2DZP optimized geometry) and $Te(OH)_4$ (*x*, C_2 symmetry, MP2/LANL2DZP optimized geometry) vs. the H−E−Te−E torsion angle (E = S for $Te(SH)_2$ and $E = O^{eq}$ for $Te(OH)_4$)[9]

The temperature dependence of $\delta(^{125}Te)$ of $Te(SMe)_2$ and $Te(S\mathit{t}Bu)_2$, which is presented in Table 3, can also be interpreted in terms of this model. A rise in temperature will lead to an increased torsional vibration around the Te−S bonds. Since electronic energy and $\delta[^{125}Te(SR)_2]$ exhibit minima for values of τ(X−S−Te−S) close to 90° (X = H, C; see Figure 1 and Figure 6 (b) further down. See also ref.[4]), thermally induced torsional vibrations will increasingly populate angles outside 90° and hence cause an increase in $\delta(^{125}Te)$.

Table 2. Physical data of the model compound $Te(SH)_2$ (C_2 symmetry) as a function of τ(HSTeS)

τ(HS^{1}TeS^2)[a]	Te−S	δ(^{125}Te)	E_{rel}	E_{HOMO}	E_{LUMO}	ΔE	E_1 [b]	E_2 [c]
0	246.0	2112	73.8	−0.29780	0.03080	0.32860	0	0
20	244.7	1876	59.6	−0.30077	0.03690	0.33767	−	17.2
40	242.5	1480	32.0	−0.30875	0.04351	0.35226	10.0	38.5
60	240.9	1217	10.5	−0.32111	0.05373	0.37484	17.9	64.4
80	240.2	1096	0.1	−0.33300	0.05565	0.38865	22.7	80.8
90	240.2	1070	0	−0.33409	0.05611	0.39020	22.9	82.5
100	240.4	1088	3.3	−0.33043	0.05631	0.38674	21.4	79.1
120	241.4	1235	17.8	−0.31659	0.04830	0.36489	14.7	59.9
140	242.9	1615	36.7	−0.30418	0.03560	0.33978	6.9	33.9
160	244.1	2117	53.1	−0.29734	0.02607	0.32341	−	14.3
180	244.6	2358	60.2	−0.29534	0.02299	0.31833	0	0

[a] E_{rel}, E_1 and E_2 in kJ·mol^{-1}, E_{HOMO}, E_{LUMO} and ΔE in Hartree, δ(^{125}Te) relative to $TeMe_2$, Te−S in pm. [b] E_1 is the second order energy for the n_p(Te)-σ*(S−H) orbital interaction in an NBO basis. n_p(Te) also interacts with ry_d(S), but the energy of this interaction is nearly independent of τ(HS^{1}TeS^2) and varies between 10.5 and 12.5 kJ·mol^{-1}. [c] E_2 is the second order energy for the n_p(S)-σ*(Te−S′) orbital interaction in an NBO basis.

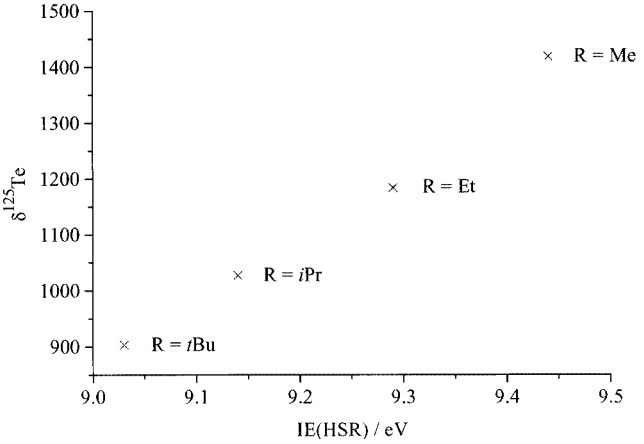

Figure 2. Experimental ^{125}Te NMR chemical shifts of $Te(SR)_2$ vs. first ionization energy of HSR (R = Me, Et, *i*Pr, *t*Bu)

Table 3. ^{125}Te NMR chemical shift of $Te(SMe)_2$ and $Te(StBu)_2$ at different temperatures

T /K	223	243	263	283	298
δ[^{125}Te(SMe)$_2$]	1395	1402	1410	1417	1423
δ[^{125}Te(S*t*Bu)$_2$]	881	885	890	896	901

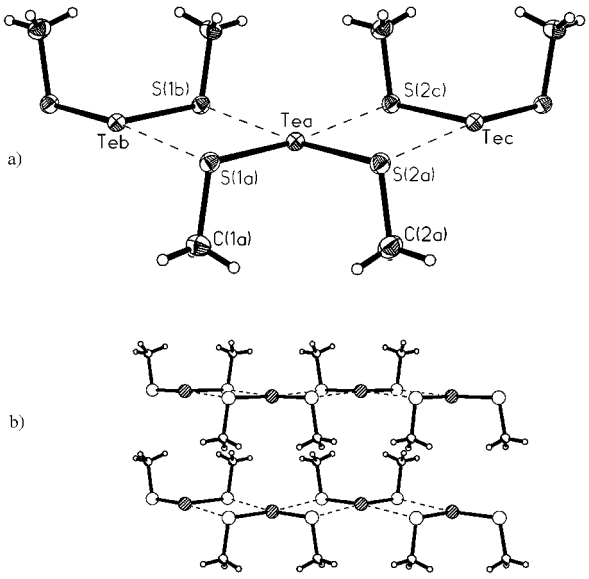

Figure 3. (a) Molecular structure and intermolecular association of *cis*-$Te(SMe)_2$ in the solid state; displacement ellipsoids are at the 50% probability level; (b) packing of chains of [*cis*-$Te(SMe)_2$]$_n$ in the solid state

Molecular and Crystal Structures

The single crystal X-ray structure of $Te(SMe)_2$ (see Figure 3, a) shows this compound to exhibit a *cis*-conformation in the solid state. It is thus different from $Te(SEt)_2$ (see Figure 4, a), $Te(SiPr)_2$, $Te(StBu)_2$ and the isovalence electronic compound $S(OCH_3)_2$, which crystallize as *trans*-conformers.[4,17] Since the energy differences between *cis*- and *trans*-conformers are similar for $Te(SMe)_2$ and $Te(SEt)_2$ (vide infra), packing effects in the crystal are seen to stabilize the *cis*-conformer in one and the *trans*-conformer in the other case. Each $Te(SMe)_2$ and each $Te(SEt)_2$ molecule forms two Te···S bonds to each of its two nearest neighbors, leading to $(TeS_2)_n$ chains in which each Te atom exhibits a distorted trapezoidal coordination (see Figure 3 and 4). In $Te(SEt)_2$, neighboring molecules in these chains exhibit enantiomeric *trans*-conformations. The average intermolecular Te···S distances and the Te−S bond lengths in $Te(SR)_2$ (R = Me, Et, *i*Pr, *t*Bu) correlate with each other, as can be seen in Figure 5: the shorter the intermolecular Te···S distances are, the longer the Te−S bonds become. This corresponds to the correlation of S−S bond lengths with intramolecular S···S distances in 6a-thiathiophthene derivatives.[18] Comparison of the MP2/LANL2DZP optimized structural parameters of monomeric *cis*-$Te(SMe)_2$ with the middle unit of [*cis*-$Te(SMe)_2]_3$ also reveals that Te···S interactions increase the Te−S bond lengths and narrow the S−Te−S angle (see Table 4). This structure correlation leads to the assumption that a σ*(Te−S) orbital is involved

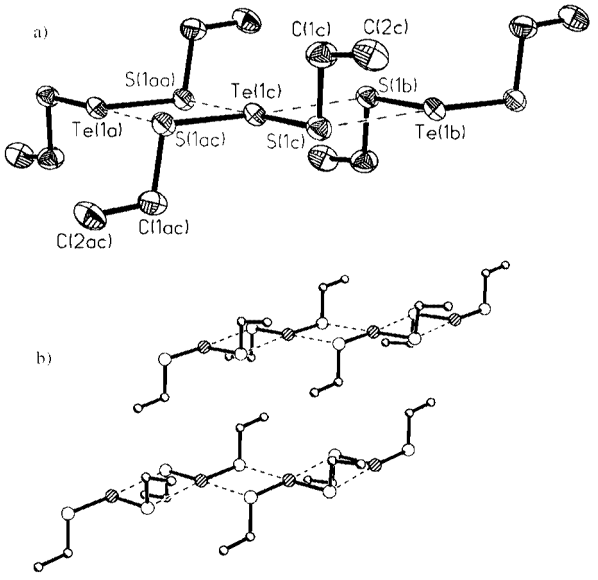

Figure 4. (a) Molecular structure and intermolecular association of $Te(SEt)_2$ in the solid state; displacement ellipsoids are at the 50% probability level; (b) packing of chains of $[trans\text{-}Te(SEt)_2]_n$ in the solid state; hydrogen atoms are omitted for clarity

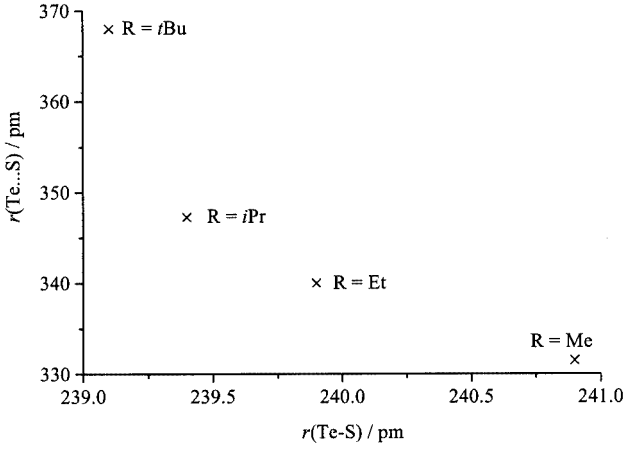

Figure 5. Intermolecular Te···S distances vs. Te−S bond lengths in the solid state structures of $Te(SR)_2$ (R = Me, Et, *i*Pr, *t*Bu); data for $Te(SiPr)_2$ and $Te(StBu)_2$ are taken from reference[4]

in the formation of the Te···S bond. An analysis of the bonding situation in the $Te(SMe)_2$ trimer in terms of natural bond orbitals shows that apart from π-type intramolecular $n_p(S)$-σ*(Te−S′) interactions (69 kJ·mol^{-1}), σ-type intermolecular $n_p(S)$-σ*(Te−S′) interactions (61 kJ·mol^{-1}) are also present. While the former are important for the Te−S bonds, the latter are essential for the Te···S interaction. These σ-type intermolecular $n_p(S)$-σ*(Te−S′) interactions explain the lengthening of the Te−S bond (transfer of electron density into an antibonding orbital) as well as the narrowing of the S−Te−S angle (reduced intramolecular repulsion of the S atoms).

Ab initio Thermochemistry

There are several constitutional isomers of $Te(SMe)_2$, some of which are given in Scheme 2 together with their calculated (MP2/LANL2DZP) relative standard enthalpies. Each of these isomers represents a minimum on the potential energy surface. The *trans*-conformers are given for isomers A and B. In isomers D and E, the Te−C and S−C bond vectors are nearly orthogonal to each other. Isomer A exhibits the lowest standard enthalpy of the entire group, hence $Te(SMe)_2$ is not only the kinetically favored product of the reaction of Te^{IV} compounds with HSMe, but is also thermodynamically more stable than the other constitutional isomers. Isomers A and B, which contain only divalent chalcogen atoms, are more stable than C−E, where one tetravalent chalcogen atom is present. Among the latter, E, which possesses a tetravalent Te atom, is more stable than C and D, which contain tetravalent S atoms. Regarding the relative stabilities of A and B, a comparison with ab initio calculations of the constitutional isomers of HSOSH is of interest.[19] Due to the larger energy of the O−H bond com-

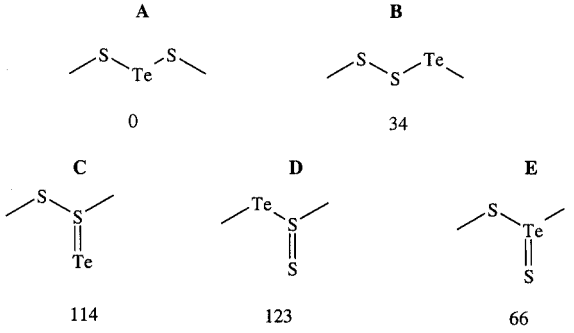

Scheme 2. Different constitutional isomers of $Te(SMe)_2$ (A) and their MP2/LANL2DZP calculated relative standard enthalpies, ΔH^{298} (kJ·mol^{-1})

Table 4. Selected parameters from ab initio optimized and solid-state structures of $Te(SMe)_2$ and $Te(SEt)_2$

	XRD		ab initio		
	$Te(SMe)_2$	$Te(SEt)_2$	$Te(SMe)_2$ [a]	$[Te(SMe)_2]_3$ [b]	$Te(SEt)_2$ [c]
Te−S/pm	240.6(1)/241.2(1)	239.9(1)	239.3	241.3	239.4
Te···S/pm	328.1(1)/334.8(1)	340.0(1)		348.5	
S−C/pm	181.3(4)/181.7(4)	182.8(5)	183.5	183.4	184.1
S−Te−S/°	98.9(1)	98.7(1)	103.4	99.4	100.2
Te−S−C/°	104.0(2)/103.5(1)	104.6(2)	102.9	102.5	101.9
τ_1/°	85.1(2)	80.6(2)	86.4	91.2	76.1
τ_2/°	−86.3(2)	80.6(2)	−86.4	−91.2	76.1

[a] C_s symmetry. [b] All three $Te(SMe)_2$ with C_s symmetry, only parameters for the middle unit are given. [c] C_2 symmetry.

pared to that of the S−H bond, the HOSSH isomer is significantly more stable than the HSOSH form. For $Te(SMe)_2$, an analogous case is assumed regarding the energies of the S−C and the Te−C bond.

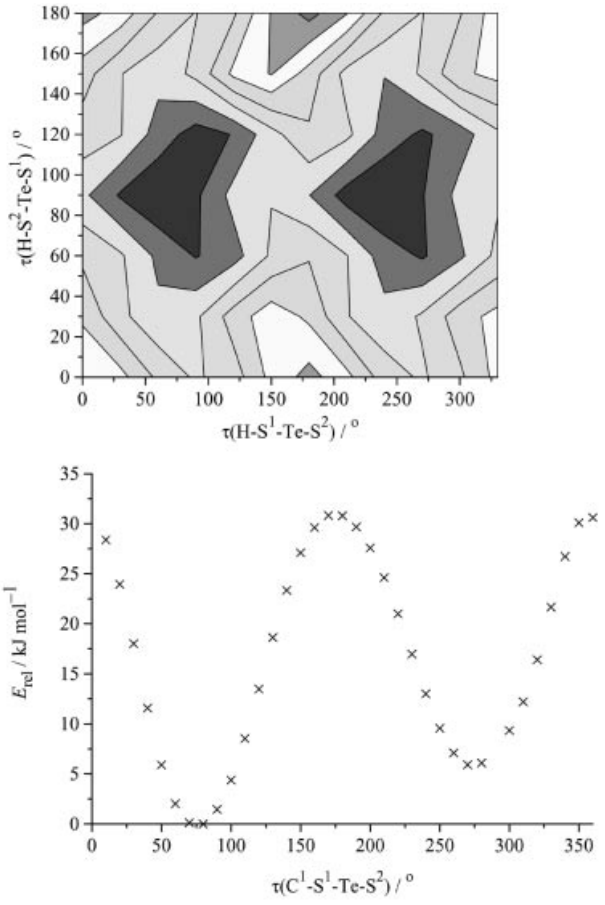

Figure 6. (a) MP2/LANL2DZP electronic energy of $Te(SH)_2$ as a function of both STeSH torsion angles; dark regions correspond to low energies and light regions to high energies; (b) MP2/LANL2DZP electronic energy of $Te(SMe)_2$ as a function of the $C^1-S^1-Te-S^2$ torsion angle; the $C^2-S^2-Te-S^1$ torsion angle was optimized freely and adopted values between 75 and 90°

As can be seen from Figure 6, part a, the model compound $Te(SH)_2$ forms stable *cis*- and *trans*-conformers. The electronic energy of *trans*-$Te(SH)_2$ [left minimum in Figure 6, part a)] is only about 1 kJ·mol^{-1} smaller than that of *cis*-$Te(SH)_2$. The C_{2v} symmetric conformation with $H-S^1-Te-S^2 = H-S^2-Te-S^1 = 180°$ represents a second-order saddle point on the potential energy surface.

Ab initio studies revealed that $Te(SMe)_2$ and $Te(SEt)_2$ also form stable *cis*- and *trans*-conformers. The electronic energies of *trans*-$Te(SMe)_2$ and *trans*-$Te(SEt)_2$ are lower than those of *cis*-$Te(SMe)_2$ and *cis*-$Te(SEt)_2$ by 6 and 5 kJ·mol^{-1}, respectively. The potential energy of $Te(SMe)_2$ as a function of one C−S−Te−S torsion angle is depicted in Figure 6, part b). The barrier between *cis*- and *trans*-$Te(SMe)_2$ amounts to about 30 kJ·mol^{-1} and should thus allow for a rapid interconversion of the two conformers at ambient temperatures.

Conclusion

Characteristic structural and ^{125}Te NMR spectroscopic features of tellurium(II) dialkanethiolates, $Te(SR)_2$, can be explained by intra- and intermolecular $n_p(S)$-σ*(Te−S′) orbital interactions. Since this orbital interaction varies significantly with the C−S−Te−S- torsion angle, the ^{125}Te NMR chemical shift of $Te(SR)_2$ shows a strong dependence on the molecular conformation. While intramolecular $n_p(S)$-σ*(Te−S′) interactions are responsible for molecular conformations, intermolecular $n_p(S)$-σ*(Te−S′) interactions play an essential role in determining the structure in the solid state. Since the orbital energies depend on the ligand, the electronic features of the tellurium atom in $Te(SR)_2$, and hence the reactivity of the compound, can be controlled by changing the nature of the alkyl group R.

Experimental Section

General Procedures: All procedures were carried out under an inert gas atmosphere or in vacuo. Solvents were purified according to standard procedures. If possible, exposure of $Te(SMe)_2$ and $Te(SEt)_2$ to daylight was avoided. Due to their thermal instability, both compounds were stored at −40 °C.

NMR: Bruker DRX 400. IR: Mattson Galaxy 2030 FTIR, resolution 4 cm^{-1}. MS: Finnigan MAT 8230. CHS analysis: Elemental Vario EL2.

$Te(SCH_3)_2$: Liquid methanethiol ($HSCH_3$; 20 mL; ρ(0 °C) = 0.87 g·mL^{-1}, 0.36 mol) was slowly transferred in the gas phase with a stream of argon into an ice-cooled suspension of tellurium dioxide (14.30 g, 89.6 mmol) in methanol (100 mL) and hydrochloric acid (0.5 mL, 37%). During the course of the reaction, the suspension at first became yellow before turning black due to precipitation of elemental tellurium. Subsequently, the solvent and all volatile reaction products were removed from the reaction mixture by low temperature distillation under reduced pressure. The crude product was extracted with petroleum ether several times and, from the combined extracts, yellow crystals of $Te(SCH_3)_2$ precipitated at −40 °C. Yield: 13.92 g (70.5%). M.p. 5 °C. $C_2H_6S_2Te$ (221.79): calcd. C 10.83, H 2.73, S 28.91; found C 10.37, H 2.35, S 27.63. MS(70 eV, EI): *m/z* (%) = 223.6 (36.4) [M^+], 176.7 (27.2) [$TeSCH_3^+$], 93.9 (100.0) [$H_3CSSCH_3^+$] ppm. ^1H NMR (400.000 MHz, C_6D_6, 25 °C, TMS): δ = 2.86 ppm. $^{13}C\{^1H\}$ NMR (100.577 MHz, C_6D_6, 25 °C, TMS): δ = 22.7 ppm. $^{125}Te\{^1H\}$ NMR (126.387 MHz, C_6D_6, 25 °C, $Te(CH_3)_2$]: δ = 1419 ppm. IR (liq., CsI): $\tilde{\nu}$ = 2981 [s, $\nu_s(CH_3)$], 2908 [vs, $\nu_{as}(CH_3)$], 2836 [m, $\nu(CH_3)$], 2815 (s, 1st overtone of 1419), 1419 [vs, $\delta(CH_3)$], 1303 [vs, $\delta(CH_3)$], 950 [vs, $\rho(CH_3)$], 688 [m, $\nu_{as}(S-C)$], 351 [s, $\nu_{as}(TeS_2)$], 331 [s, $\nu_s(TeS_2)$] cm^{-1}.

$Te(SCH_2CH_3)_2$: Tellurium(IV) tetraisopropoxide [$Te(OiPr)_4$; 1.18 g, 3.2 mmol) dissolved in petroleum ether (10 mL) was slowly added to a stirred solution of ethanethiol ($HSCH_2CH_3$; 0.82 g, 13.2 mmol) in petroleum ether (10 mL) at −78 °C. During this procedure the initally colorless solution turned yellow. Subsequently, the solvent and all volatile compounds were distilled in vacuo and the remaining yellow solid was dissolved in petroleum ether. From this solution yellow crystals of $Te(SCH_2CH_3)_2$ precipitated at −40 °C which were dried in vacuo. Yield: 0.76 g (95.0%). M. p. 18−20 °C. $C_4H_{10}S_2Te$ (249.84): calcd. C 19.23, H 4.03, S 25.66; found C 19.25, H 4.01, S 25.57. MS (70 eV, EI): *m/z* (%) = 251.9 (58.8)

Table 5. Crystal data for $Te(SMe)_2$ and $Te(SEt)_2$

[a]	$Te(SMe)_2$	$Te(SEt)_2$
Empirical formula	$C_2H_6S_2Te$	$C_4H_{10}S_2Te$
FW/g mol^{-1}	221.79	249.84
Crystal system	triclinic	monoclinic
Space group	$P\bar{1}$	$C2/c$
Z	2	4
Temperature/K	133(2)	193
$\rho_{calcd.}$/g cm^{-3}	2.382	1.99
μ/mm^{-1}	5.337[b]	3.97[c]
$F(000)$	204	472
Crystal size	0.40 × 0.20 × 0.20 mm	0.05 × 0.26 × 1.00 mm
θ-range	2.56 to 35.02°	2.8 to 28.3°
Limiting indices	$-8 \le h \le 8$	$-15 \le h \le 17$
	$-12 \le k \le 12$	$-11 \le k \le 10$
	$-13 \le l \le 13$	$-11 \le l \le 8$
a/Å	5.2828(5)	13.2228(4)
b/Å	7.480(1)	8.9408(3)
c/Å	8.256(1)	8.4005(3)
α/deg	105.12(1)	90.0
β/deg	90.19(1)	122.909(2)
γ/deg	100.51(1)	90.00
V/Å^3	309.21(8)	833.77(6)
Reflections measured	5408	8130
Unique reflections	2705	1026
Refl. $\|F\| > 4\sigma(F)$	2705	996
R [$\|F\| > 4\sigma(F)$][d]	0.0491	0.0355
Goodness-of-fit on F^2	1.108	1.074
Largest diff. peak and hole	7.10 and −3.12 e·Å^{-3} [e]	2.26 and −1.00 e·Å^{-3}

[a] Mo-K_α radiation with $\lambda = 0.71069$ Å was used. [b] Absorption correction with DELABS.[20] [c] Absorption correction with MULABS.[21] [d] $R = \Sigma \, ||F_o| - |F_c|| / \Sigma \, |F_o|$. [e] Maximum and minimum are 86 pm and 79 pm, respectively, away from the Te atom.

[M^+], 188.9 (19.1) [$TeSEt^+$], 159.8 (20.0) [TeS^+], 122.0 (29.2) [$EtSSEt^+$]. ^{1}H NMR (400.000 MHz, C_6D_6, 25 °C, TMS): δ = 1.14 (t, $^3J_{H,H}$ = 7.3 Hz, 3 H, CH_3), 2.85 (q, $^3J_{H,H}$ = 7.3 Hz, 2 H, CH_2) ppm. $^{13}C\{^1H\}$ NMR (100.577 MHz, C_6D_6, 25 °C, TMS): δ = 17.7 (CH_3), 32.4 (CH_2) ppm. $^{125}Te\{^1H\}$ NMR (126.387 MHz, C_6D_6, 25 °C, $Te(CH_3)_2$]: δ = 1184 ppm. IR (liq., CsI): $\tilde{\nu}$ = 2962 [vs, $\nu_s(CH_3)$], 2955 [vs, $\nu_s(CH_3)$], 2919 [vs, $\nu_{as}(CH_2)$], 2862 [s, $\nu_{as}(CH_3)$], 2821 [m, $\nu_s(CH_2)$], 1445 [vs, $\delta_{as}(CH_3)$], 1420 [s, $\delta(CH_2)$], 1371 [vs, $\delta_s(CH_3)$], 1268 (sh), 1248 [vs, $\delta(CH_2)$], 1116 (sh), 1099 (s), 1045 [s, $\rho(CH_3)$], 1024 (s), 966 (s), 758 [s, $\rho(CH_3)$], 657 (w), 638 [m, ν(S−C)], 539 (w), 515 (w), 392 [m, δ(S−C)], 361 [s, ν_{as}(Te−S)], 329 [s, ν_s(Te−S)], 263 (m) cm^{-1}.

Crystal Structure Determination: Diffraction experiments for $Te(SMe)_2$ were performed on a Nonius-Turbo-CAD4 diffractometer. Its crystal structure was solved by direct methods and structural refinement against F^2 (SHELXTL 5.01).[22]

Diffraction experiments for $Te(SEt)_2$ were performed on a BRUKER Nonius CCD diffractometer. Its crystal structure was solved by direct methods and structural refinement was F^2 (SHELXL 97).[23] Details of the crystal structure determination of $Te(SMe)_2$ and $Te(SEt)_2$, as well as their crystal data, are given in Table 5.

CCDC-170962 and CCDC-191964 contain the supplementary crystallographic data for this paper. These data can be obtained free of charge via www.ccdc.cam.ac.uk/conts/retrieving.html (or from the Cambridge Crystallographic Data Centre,12 Union Road, Cambridge CB2 1EZ, UK; fax: (+44)1223−336−033; or E-mail: deposit@ccdc.cam.ac.uk).

Theoretical Methods: Quantum chemical ab initio investigations were performed with the Gaussian 94 and Gaussian 98 program packages.[24,25] Optimization of molecular geometries, calculation of vibrational frequencies and an analysis of the electronic structure in terms of natural orbitals [12,13] was performed at the MP2 level, with an effective core double-zeta valence basis set,[26] augmented by appropriate polarization functions for Te, S (with exponents according to Höllwarth et al. [27]), and C (exponent 0.75), the basis set being designated as LANL2DZP. Applied symmetry restrictions are given in the text. Calculated vibrational frequencies, scaled by a factor 0.96, were used to assign the IR signals. NMR shielding tensors were calculated according to the GIAO method[28] by using density functional theory (B3LYP) [29] and the IGLO-II basis set,[30] together with an MP2/LANL2DZP optimized molecular geometry.

Acknowledgments

We thank Prof. Dr. M. Kaupp (Universität Würzburg) for his support concerning the calculation of NMR shifts.

[1] Out of 34 solid-state molecular structures with noncyclic $CE^1E^2E^3C$ units found in the Cambridge crystallographic data base, $S(S_2COCH_3)$ and $Se(S_2COCH_3)$ are the only examples exhibiting a *cis*-conformation (see ref.[2]).

[2] N. J. Brøndmo, S. Esper Ås, S. Husebye, *Acta Chem. Scand., Ser. A* **1975**, *29*, 93−104.

[3] R. E. Allan, H. Gornitzka, J. Kärcher, M. A. Paver, M.-A. Rennie, C. A. Russell, P. R. Raithby, D. Stalke, A. Steiner, D. W. Wright, *J. Chem. Soc., Dalton Trans.* **1996**, 1727−1730.

[4] H. Fleischer, S. Stauf, D. Schollmeyer, *Inorg. Chem.* **1999**, *38*, 3725−3729.

[5] H. Fleischer, D. Schollmeyer, *Angew. Chem.* **2000**, *112*, 3840−3842; *Angew. Chem. Int. Ed.* **2000**, *39*, 3705−3706.

[6] R. Steudel, *Angew. Chem.* **1975**, *87*, 683−692; *Angew. Chem. Int. Ed. Engl.* **1975**, *14*, 655−664.
[7] M. Liedtke, A. H. Saleck, K. M. T. Yamada, G. Winnewisser, D. Cremer, E. Kraka, A. Dolgner, J. Hahn, S. Dobos, *J. Phys. Chem.* **1993**, *97*, 11204−11210.
[8] H. Fleischer, D. Schollmeyer, *Inorg. Chem.* **2002**, *41*, 4739−4747.
[9] Since no relativistic effects were included in the calculation of the nuclear shielding constants, there are considerable differences between calculated and experimental ^{125}Te NMR chemical shifts. It was previously shown (Y. Ruiz-Morales, G. Schreckenbach, T. Ziegler, *J. Phys. Chem. A* **1997**, *101*, 4121−4127) that calculations neglecting the spin-orbit-induced contributions to nuclear shielding still give ^{125}Te chemical shifts which are in good agreement with experimental values. In the present case, the experimentally observed trends of $\delta[^{125}Te(SR)_2]$ with R are at least well reproduced.
[10] H. Fleischer, D. Schollmeyer, *Inorg. Chem.* **2001**, *40*, 324−328.
[11] D. B. Denney, D. Z. Denney, P. J. Hammond, Y. F. Hsu, *J. Am. Chem. Soc.* **1981**, *103*, 2340−2347.
[12] A. E. Reed, R. B. Weinstock, F. Weinhold, *J. Chem. Phys.* **1985**, *83*, 735−746.
[13] A. E. Reed, L. A. Curtiss, F. Weinhold, *Chem. Rev.* **1988**, *88*, 899−926.
[14] R. K. Harris, *Nuclear Magnetic Resonance − A Physicochemical View*, Longman Scientific & Technical, Harlow, **1986**.
[15] T. A. Koopmans, *Physica* **1934**, *1*, 104−113.
[16] It is assumed that the differences in ionization energies and thus in $E[n_p(S)]$ between various thiols are reflected in different $E[n_p(S)]$ values for the corresponding tellurium(II) dithiolates.
[17] J. Buschmann, P. Luger, R. Koritsanszky, H. Schmidt, R. Steudel, *J. Phys. Chem.* **1992**, *96*, 9243−9250.
[18] H.-B. Bürgi, *Angew. Chem.* **1975**, *87*, 461−496; *Angew. Chem. Int. Ed. Engl.* **1975**, *14*, 460−
[19] R. Steudel, Y. Drozdova, R. H. Hertwig, W. Koch, *J. Phys. Chem.* **1995**, *99*, 5319−5324.
[20] A. L. Spek, *Acta Crystallogr., Sect. A* **1990**, *46*, C-34.
[21] R. Blessing, *Acta Crystallogr., Sect. A* **1995**, *51*, 33−38.
[22] SHELXTL PC version 5.01, Siemens Analytical X-ray Instruments, Inc., Madison, WI, **1994**.
[23] G. M. Sheldrick, SHELXL-97, *Program for crystal structure refinement*, Universität Göttingen, Göttingen (Germany), **1996**.
[24] Gaussian 94, Revision E.1, M. J. Frisch, G. W. Trucks, H. B. Schlegel, P. M. W. Gill, B. G. Johnson, M. A. Robb, J. R. Cheeseman, T. Keith, G. A. Petersson, J. A. Montgomery, K. Raghavachari, M. A. Al-Laham, V. G. Zakrzewski, J. V. Ortiz, J. B. Foresman, J. Cioslowski, B. B. Stefanov, A. Nanayakkara, M. Challacombe, C. Y. Peng, P. Y. Ayala, W. Chen, M. W. Wong, J. L. Andres, E. S. Replogle, R. Gomperts, R. L. Martin, D. J. Fox, J. S. Binkley, D. J. Defrees, J. Baker, J. P. Stewart, M. Head-Gordon, C. Gonzalez, J. A. Pople, Gaussian, Inc., Pittsburgh PA, **1995**.
[25] Gaussian 98, Revision A.6, M. J. Frisch, G. W. Trucks, H. B. Schlegel, G. E. Scuseria, M. A. Robb, J. R. Cheeseman, V. G. Zakrzewski, J. A. Montgomery, Jr., R. E. Stratmann, J. C. Burant, S. Dapprich, J. M. Millam, A. D. Daniels, K. N. Kudin, M. C. Strain, O. Farkas, J. Tomasi, V. Barone, M. Cossi, R. Cammi, B. Mennucci, C. Pomelli, C. Adamo, S. Clifford, J. Ochterski, G. A. Petersson, P. Y. Ayala, Q. Cui, K. Morokuma, D. K. Malick, A. D. Rabuck, K. Raghavachari, J. B. Foresman, J. Cioslowski, J. V. Ortiz, B. B. Stefanov, G. Liu, A. Liashenko, P. Piskorz, I. Komaromi, R. Gomperts, R. L. Martin, D. J. Fox, T. Keith, M. A. Al-Laham, C. Y. Peng, A. Nanayakkara, C. Gonzalez, M. Challacombe, P. M. W. Gill, B. Johnson, W. Chen, M. W. Wong, J. L. Andres, C. Gonzalez, M. Head-Gordon, E. S. Replogle, and J. A. Pople, Gaussian, Inc., Pittsburgh PA, **1998**.
[26] W. R. Wadt, P. J. Hay, *J. Chem. Phys.* **1985**, *82*, 284−298.
[27] A. Höllwarth, M. Böhme, S. Dapprich, A. W. Ehlers, A. Gobbi, V. Jonas, K. F. Köhler, R. Stegmann, A. Veldkamp, G. Frenking, *Chem. Phys. Lett.* **1993**, *208*, 237−240.
[28] K. Wolinski, J. F. Hinton, P. Pulay, *J. Am. Chem. Soc.* **1992**, *112*, 8251−8260.
[29] A. D. Becke, *J. Chem. Phys.* **1993**, *98*, 5648−5652.
[30] W. Kutzelnigg, U. Fleischer, M. Schindler, *NMR-Basic Principles and Progress*, Vol. 23, Springer-Verlag, Heidelberg, **1990**.

Received August 20, 2002
[I02470]